

Photoinduced Electron-Transfer and Electron-Mediating Processes of Fullerenes and Phenothiazine Oligomers in a Polar Solvent

D.-M. Shafiqul Islam,[1,†] Yoshiko Sasaki,[1] Hidehito Kawauchi,[2] Masatoshi Kozaki,[2] Yasuyuki Araki,*[1] Osamu Ito,[1] and Keiji Okada*[2]

[1]Institute of Multidisciplinary Research for Advanced Materials, Tohoku University, Katahira, Aoba-ku, Sendai 980-8577

[2]Department of Chemistry, Graduate School of Science, Osaka City University, Sugimoto, Sumiyoshi-ku, Osaka 558-8585

Received August 24, 2007; E-mail: araki@tagen.tohoku.ac.jp

Photoinduced electron transfer between fullerenes (C_{60} and C_{70}) and three phenothiazine oligomers ((PTZ)$_n$s; $n = 1$, 2, and 3) was studied by using a transient absorption method in the visible and near-IR regions. Electron transfer took place from (PTZ)$_n$s to the triplet states of fullerenes ($^3C_{60}$* and $^3C_{70}$*), giving the radical anions of fullerenes ($C_{60}^{\bullet-}$ and $C_{70}^{\bullet-}$) and the radical cations of (PTZ)$_n$s, which exhibited strong absorptions in visible and near-IR region for $n = 2$ and 3. From these absorptions, positions of the radical cation in (PTZ)$_2^{\bullet+}$ and (PTZ)$_3^{\bullet+}$ generated by electron donation were also determined. Rate constants and quantum efficiencies of the electron transfer were found to be quite high, because of the strong electron-donating abilities of (PTZ)$_n$s; the order of the rates of electron transfer to $^3C_{60}$* and $^3C_{70}$* is (PTZ)$_1$ > (PTZ)$_2$ = (PTZ)$_3$, which corresponds to the decreasing order of their oxidation potentials. Upon addition of hexylviologen dication (HV^{2+}), an electron-mediating process occurred from $C_{60}^{\bullet-}$ to HV^{2+}, yielding the viologen radical cation ($HV^{\bullet+}$). In the presence of a sacrificial donor, $HV^{\bullet+}$ persisted for a long time.

Fullerenes, such as C_{60} and C_{70}, have been well established as electron acceptors in photoinduced electron-transfer processes with electron donors.[1–4] In these systems, the excited singlet states and/or triplet states of the fullerenes accept electrons from the ground states of electron donors,[5–7] although the relative contribution of the singlet states and the triplet states varies with the concentration of the electron donors.[8–10] Because of high degree of delocalization of the π-electrons in fullerenes, the transient absorption bands of the excited singlet states ($^1C_{60}$* and $^1C_{70}$*), the triplet states ($^3C_{60}$* and $^3C_{70}$*), and the anion radicals ($C_{60}^{\bullet-}$ and $C_{70}^{\bullet-}$) have been reported to appear in the vis and near-IR regions.[1–10] Thus, it is important to obtain the spectral and kinetic information on the transient species in the vis and near-IR regions in order to clarify the mechanism.

On the other hand, phenothiazine derivatives are well-known heterocyclic compounds with a strong electron-donor ability, because of their eight π and n-electrons in the central ring.[11–14] Phenothiazine molecules, oligomers, and polymers have recently attracted much research interest, because of their potential applicability in light-emitting diodes, field effect transistors, and photovoltaic cells.[15–21] In the present study, we employed three phenothiazine oligomers, (PTZ)$_n$s ($n = 1$, 2, and 3 in Scheme 1). Although (PTZ)$_1$ is a good donor for the electron-transfer processes, the radical cation (PTZ)$_1^{\bullet+}$ shows rather weak absorptions in visible region.[22] However, we have recently found that the trimer radical cation (PTZ)$_3^{\bullet+}$ exhibits a strong charge-transfer (CT) absorption band in the near-IR region.[23] The structure of (PTZ)$_3^{\bullet+}$ has been found to be considerably different from the neutral state, i.e., a large geometrical change due to the rotation of the outer PTZ rings is accompanied by a hole localization onto the central PTZ ring during the one-electron chemical oxidation of (PTZ)$_3$.[23] In the course of the photoinduced electron transfer studies using nanosecond laser photolysis, conformation changes could be observed, if the they were much slower than the nanosecond timescale. Therefore, the present study has the following purposes: 1) establishing the photoelectron-transfer processes of fullerenes with these (PTZ)$_n$s$^{\bullet+}$, including an estimation of the rate constants and the quantum yields, 2) gaining insight into the geometrical changes in (PTZ)$_n$s$^{\bullet+}$, and 3) applying this electron-transfer process to a electron-mediating system using an electron-mediating reagent.[7–9] In the electron-transfer/electron-mediating system in the presence of hexylviologen dication (HV^{2+}), a long-lived hexylviologen radical cation ($HV^{\bullet+}$) was observed in the presence of an appropriate sacrificial donor, demonstrating that this is an efficient photosensitizing electron-transfer/electron-mediating system, composed of C_{60}/C_{70} and (PTZ)$_n$s in a polar solvent.

Results and Discussion

Steady-State UV–Vis Spectra. The steady-state absorption spectra of (PTZ)$_2$, C_{60}, and a mixture of them are shown in Fig. 1. The absorption spectrum of the mixture of C_{60} with (PTZ)$_2$ is almost equal to the sum of the components. A similar absorption spectral behavior was also found in the case of (PTZ)$_1$ and (PTZ)$_3$. This finding suggests that no appreciable

† Present address: Department of Chemistry, Jahangirnagar University, Savar, Dhaka-1342, Bangladesh

Published on the web January 10, 2008; doi:10.1246/bcsj.81.103

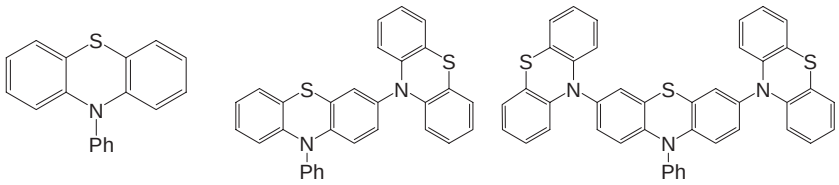

10-Phenylphenothiazine **(PTZ)$_1$**

3-(10-Phenothiazinyl)-phenothiazine **(PTZ)$_2$**

3,7-Bis(10-phenothiazinyl)-10-phenylphenothiazine **(PTZ)$_3$**

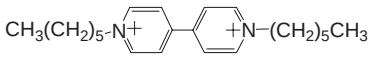

Hexylviologen (HV^{2+})

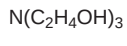

2,2',2"-Nitrilotriethanol (NTET)

Scheme 1. Molecular structures of phenothiazine oligomers $(PTZ)_n$s, hexylviologen dication, and nitriloethanol employed in the present study.

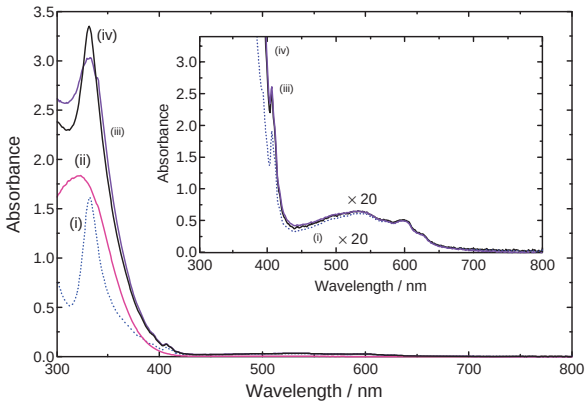

Fig. 1. Steady-state absorption spectra of (i) C_{60} (0.35 mmol dm^{-3}), (ii) $(PTZ)_2$ (0.25 mmol dm^{-3}), (iii) their mixture, and (iv) summation of (i) and (ii) in PhCN. Inset: Expanded spectra in the visible region.

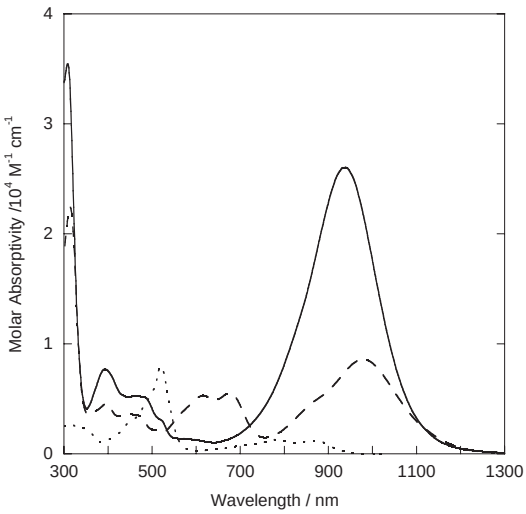

Fig. 2. Steady-state absorption spectra of $(PTZ)_1^{\bullet+}$ (···), $(PTZ)_2^{\bullet+}$ (– –), and $(PTZ)_3^{\bullet+}$ (—) in CH_2Cl_2 observed by one-electron oxidation of $(PTZ)_n$ with $TBPA^+PF_6^-$.

Table 1. Observed Absorption Maxima λ_{max} (ε) and Calculated λ_{calc} for $(PTZ)_n^{\bullet+}$

Compounds	λ_{max} (ε[a]) in CH_2Cl_2	λ_{max} in PhCN[b]	Longest λ_{calc}[c]
$(PTZ)_1^{\bullet+}$	517 nm (9540)	520 nm	772 nm
	745 nm (1410)	781 nm	
	880 nm (1320)	869 nm	
$(PTZ)_2^{\bullet+}$	990 nm (10600)	980 nm	1018 nm
$(PTZ)_3^{\bullet+}$	945 nm (28300)	939 nm	954 nm

a) ε in cm^{-1} mol^{-1} dm^3. b) The radical cations are slowly decolorized in PhCN. c) Calculated with ab initio TD-UB3lyp/6-31G(d) method.

electronic interaction exists between C_{60} and $(PTZ)_n$ in the ground state. Laser light with a wavelength of 532 nm, used for laser flash photolysis, predominantly excites C_{60}, because $(PTZ)_n$s do not absorb the light. For C_{70}, similar results to C_{60} were obtained.

The radical cations $(PTZ)_1^{\bullet+}$ and $(PTZ)_3^{\bullet+}$ were prepared by treating $(PTZ)_n$ with tris-*p*-bromophenylaminium hexafluorophosphate ($TBPA^+PF_6^-$), as previously described.[21,23] The absorption spectrum of $(PTZ)_2^{\bullet+}$, prepared similarly, is shown along with those of $(PTZ)_1^{\bullet+}$ and $(PTZ)_3^{\bullet+}$ in Fig. 2. The main absorption peaks, which appeared in CH_2Cl_2 and PhCN solutions, are summarized in Table 1.

It should be noted that the absorption peaks of $(PTZ)_2^{\bullet+}$ ($\lambda_{max} = 980$ nm in PhCN) and $(PTZ)_3^{\bullet+}$ ($\lambda_{max} = 939$ nm) appear in a longer wavelength region than that of $(PTZ)_1^{\bullet+}$ ($\lambda_{max} = 517$ nm). In our previous paper, the absorption band

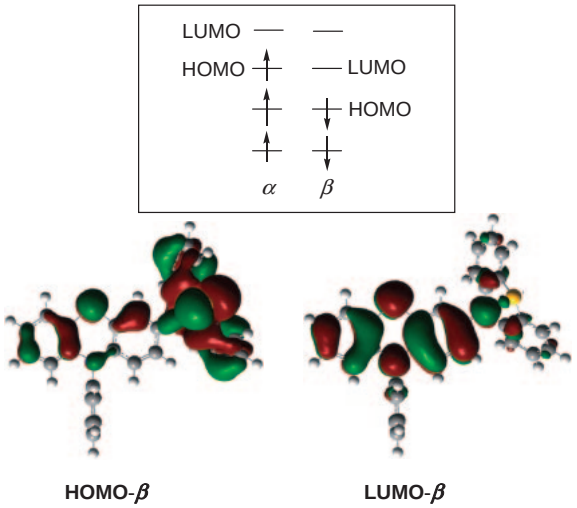

Fig. 3. (Upper panel) MO energy diagram of $(PTZ)_2^{\bullet+}$ in UHF representation. (Lower panel) optimized structure and MO shapes of the HOMO-β and the LUMO-β for $(PTZ)_2^{\bullet+}$.

Table 2. Oxidation Potentials (E_{ox}) of $(PTZ)_n$s and Free-Energy Changes (ΔG^o_{ET}) of Electron Transfer from $(PTZ)_n$s to $^3C_{60}$* and $^3C_{70}$*

Donors	E_{ox}/V vs. Ag/Ag$^+$	$-\Delta G^o_{ET}$/eV via $^3C_{60}$*	$-\Delta G^o_{ET}$/eV via $^3C_{70}$*
$(PTZ)_1$	0.38	0.79	0.80
$(PTZ)_2$	0.27	0.90	0.91
$(PTZ)_3$	0.21	0.96	0.97

of $(PTZ)_3^{\bullet+}$ in the near-IR region has been attributed to the electronic transition from the neutral terminal PTZ unit to the central $PTZ^{\bullet+}$ unit in $(PTZ)_3^{\bullet+}$ by using structural determination and theoretical calculations.[23] In the present study, to obtain the optimized structure of $(PTZ)_2^{\bullet+}$ using UB3LYP/6-31G(d) calculations,[24] we used a partial structure of the reported X-ray structure of $(PTZ)_3^{\bullet+}$ as a starting structure. In the optimized structure of $(PTZ)_2^{\bullet+}$, as shown in Fig. 3, the left PTZ ring was flat, whereas the right PTZ ring was in a butterfly structure. Then, assignment of the absorption spectra was performed on the basis of molecular orbital calculations using the TD-method involved in the Gaussian 03 program package.[24] The calculated values ($\lambda_{calcd} = 1018$ nm for $(PTZ)_2^{\bullet+}$), which were based on the transition mainly from the HOMO-β to the LUMO-β roughly, are similar to the observed value ($\lambda_{max} \approx 980$ nm). The HOMO-$\beta \rightarrow$ LUMO-β transition involves a charge-transfer transition from the right PTZ ring to the left $PTZ^{\bullet+}$ ring (Fig. 3). For $(PTZ)_1^{\bullet+}$, λ_{calcd} (=770 nm) is similar to the vibronic bands in the long wavelength region, as listed in Table 1, although these absorptions are obviously minor peaks compared to the main band at 520 nm.

Electrochemistry and Free-Energy Changes. The first oxidation potentials (E_{ox} vs. Ag/AgCl) obtained from reversible waves of cyclic voltammograms of these $(PTZ)_n$s are summarized in Table 2. The electron-donating ability of $(PTZ)_n$s increases as n increases; the oxidation potential varied from +0.21 V for $(PTZ)_3$ to +0.38 V for $(PTZ)_1$. Thus, the free-energy change of electron-transfer (ΔG^o_{ET}) via $^3C_{60}$*/$^3C_{70}$*

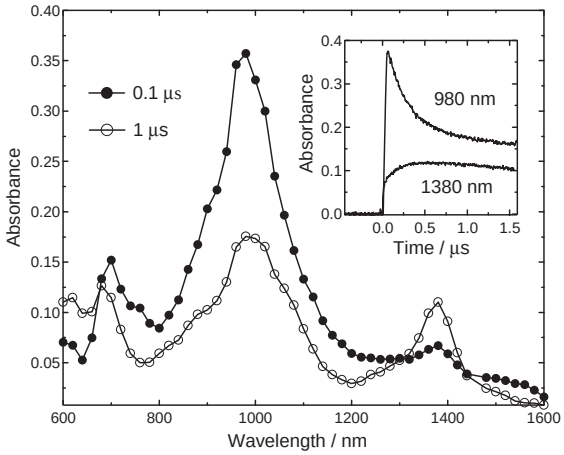

Fig. 4. Transient absorption spectra obtained by exciting with 532 nm laser light of C_{70} (0.1 mmol dm^{-3}) in the presence of $(PTZ)_2$ (1.0 mmol dm^{-3}) in Ar-saturated PhCN. Inset: Time profiles at 980 and 1380 nm.

can be calculated from E_{ox} of $(PTZ)_n$s, the first reduction potentials (E_{red}) of C_{60}/C_{70}, and the energy level of the excited triplet state (E_T) of C_{60}/C_{70} using the Rehm–Weller Eq. 1:[25]

$$\Delta G^o_{ET} = e(E_{ox} - E_{red}) - E_T - E_c. \quad (1)$$

Here, the following values were employed: $E_T = 1.56$ eV for $^3C_{60}$* and $E_T = 1.53$ eV for $^3C_{70}$*, $E_{red} = -0.45$ V for C_{60} and $E_{red} = -0.41$ V for C_{70},[26,27] $E_{ox} = 0.38$–0.21 V for the $(PTZ)_n$s (Table 2) and the Coulomb energy, $E_c = 0.06$ eV in PhCN.[5] The ΔG^o_{ET} values thus calculated are listed in Table 1; all ΔG^o_{ET} values were sufficiently negative for the nearly diffusion-controlled rate constants of the electron-transfer processes. The order of these $-\Delta G^o_{ET}$ values reflects the order of the E_{ox} values of the $(PTZ)_n$s.

Transient Absorption Spectra and Electron-Transfer Route. Nanosecond transient absorption spectra observed after laser excitation of C_{70} in the presence of $(PTZ)_2$ in PhCN are shown in Fig. 4. The absorption band of $^3C_{70}$* at 980 nm,[28–31] which appeared immediately after excitation, began to decay in the presence of $(PTZ)_2$. Along with the decay of $^3C_{70}$*, the absorption intensity at 1380 nm increased, indicating that $C_{70}^{\bullet-}$ is formed from $^3C_{70}$* by accepting an electron from $(PTZ)_2$. The absorption bands around 800–1100 nm remaining after the decay of $^3C_{70}$* were attributed to $(PTZ)_2^{\bullet+}$ from a comparison with the steady-state absorption spectra of $(PTZ)_2^{\bullet+}$. In the case of C_{60} and $(PTZ)_2$, a similar conclusion was drawn from the transient spectra, in which the $C_{60}^{\bullet-}$ band at 1080 nm overlapped with $(PTZ)_2^{\bullet+}$. For $(PTZ)_3$, a band at 960 nm due to $(PTZ)_3^{\bullet+}$ was observed. In the case of $(PTZ)_1$, a weak band at 520 nm of $(PTZ)_1^{\bullet+}$ was observed in addition to bands for $C_{60}^{\bullet-}$ and $C_{70}^{\bullet-}$.[12,14] It should be noted that the transient absorption spectra of $(PTZ)_2^{\bullet+}$ and $(PTZ)_3^{\bullet+}$ are almost the same as the steady-state absorption spectra in Fig. 2, which suggests that the positions of the radical cation in $(PTZ)_2^{\bullet+}$ and $(PTZ)_3^{\bullet+}$ after electron donation (100 ns in Fig. 4) are the same as those of the most stable radical cation in the steady state. The hole localizes mainly on the left PTZ moiety of $(PTZ)_2^{\bullet+}$ (Fig. 3), and it localizes mainly on the central PTZ moiety of $(PTZ)_3^{\bullet+}$.[21,23]

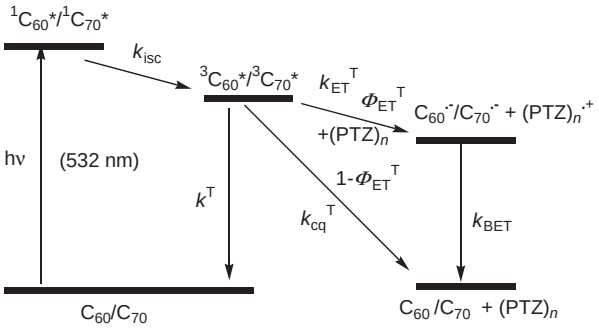

Scheme 2. Energy diagram for electron transfer via $^3C_{60}$* and $^3C_{70}$* from $(PTZ)_n$s.

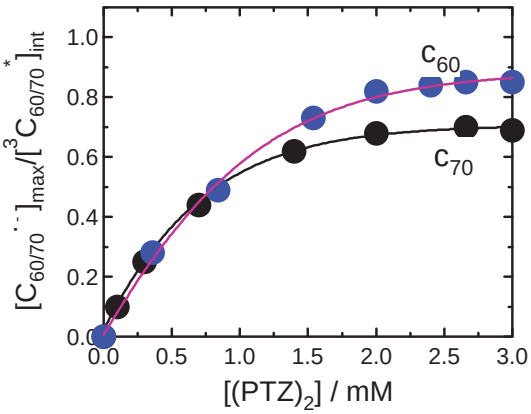

Fig. 5. Plots of efficiencies of electron transfer $[C_{60}^{\bullet-}]_{max}/[^3C_{60}^*]_{int}$ and $[C_{70}^{\bullet-}]_{max}/[^3C_{70}^*]_{int}$ vs. $[(PTZ)_2]$; mM = 10^{-3} mol dm^{-3}.

Table 3. Rate Constants and Quantum Yields

Donors	Fullerenes	k_q^T /mol^{-1} dm^3 s^{-1}	Φ_{ET}^T	k_{ET}^T /mol^{-1} dm^3 s^{-1}	k_{BET} /mol^{-1} dm^3 s^{-1}
$(PTZ)_1$	$^3C_{60}$*	3.7×10^9	0.88	3.3×10^9	2.8×10^{10}
	$^3C_{70}$*	3.6×10^9	0.70	2.5×10^9	1.3×10^{10}
$(PTZ)_2$	$^3C_{60}$*	1.4×10^9	0.89	1.3×10^9	1.4×10^{10}
	$^3C_{70}$*	1.1×10^9	0.72	7.9×10^8	1.2×10^{10}
$(PTZ)_3$	$^3C_{60}$*	1.7×10^9	0.91	1.5×10^9	1.1×10^{10}
	$^3C_{70}$*	8.8×10^8	0.73	6.4×10^8	8.1×10^9

The time profiles for the decay of $^3C_{70}$* at 980 nm and the rises of $C_{70}^{\bullet-}$ at 1380 nm are shown in the inset of Fig. 4. The initial decay curve of $^3C_{70}$* and rise curve of $C_{70}^{\bullet-}$ are almost mirror images of each other, supporting the conclusion that electron transfer takes place via $^3C_{70}$* as shown in energy diagram in Scheme 2, in which k_{isc}, k_{ET}^T, k_{cq}^T, and k_{BET} are the rate constants of the intersystem crossing, electron transfer, and collisional quenching via $^3C_{60}$*/$^3C_{70}$*, and back electron transfer, respectively. The observed slow increases in the band for $C_{70}^{\bullet-}$ indicates clearly that electron transfer does not take place via $^1C_{70}$*.[10,11]

Each decay of $^3C_{70}$* obeys first-order kinetics (Fig. 4), yielding the first-order rate constant (k_{1st}). In the absence of $(PTZ)_n$, k_{1st} equals k^T, which is 10^4 s^{-1}. The k_{1st} values increased linearly with the concentration of $(PTZ)_n$. In the presence of $(PTZ)_n$, the values of k_{1st} are in the range of 10^6–10^7 s^{-1}. The second-order quenching rate constants ($k_q^T = k_{cq}^T + k_{ET}^T$) of $^3C_{60}$*/$^3C_{70}$* for each $(PTZ)_n$ were obtained from the slopes of the pseudo-first-order plots and are listed in Table 3. These k_q^T values did not vary much with each $(PTZ)_n$, falling in the narrow range. These values are slightly smaller than the diffusion-controlled limit, $k_{diff} = 5.2 \times 10^9$ mol^{-1} dm^3 s^{-1} in PhCN.[32]

Quantum Yields and Rate Constants for Electron Transfer. In the case of systems containing C_{60} and $(PTZ)_n$s, the efficiency of electron transfer via $^3C_{60}$* can be obtained from the ratio of $[C_{60}^{\bullet-}]_{max}/[^3C_{60}^*]_{int}$, of which $[^3C_{60}^*]_{int}$ is the initial concentration of $^3C_{60}$* determined by the maximum absorbance of $^3C_{60}$* at 740 nm with a molar absorptivity, ε, of 12000 cm^{-1} mol^{-1} dm^3,[26,27] and $[C_{60}^{\bullet-}]_{max}$ is the maximum concentration of $C_{60}^{\bullet-}$ obtained from the maximum absorbance of $C_{60}^{\bullet-}$ at 1080 nm ($\varepsilon = 14000$ cm^{-1} mol^{-1} dm^3).[26,27] For $(PTZ)_2$ and $(PTZ)_3$, since their radical cation absorptions overlap with $C_{60}^{\bullet-}$ at 1080 nm, $[C_{60}^{\bullet-}]_{max}$ must be evaluated after subtracting the radical cation contribution by using the ε values at 1080 nm (see Fig. 2 and Table 1). As shown in Fig. 5, the ratios showed saturation with an increase in the concentration of the $(PTZ)_n$s. At a sufficiently high concentration of $(PTZ)_n$s (ca. 3 mmol dm^{-3}), the efficiency becomes equal to the quantum yield (Φ_{ET}^T) of the electron-transfer process via $^3C_{60}$* (Table 3). The observed values of Φ_{ET}^T for the three $(PTZ)_n$s are almost identical. Similar behavior was observed for C_{70}, as shown in Fig. 5, in which $[^3C_{70}^*]_{int}$ was determined by subtracting the absorbance of $(PTZ)_2^{\bullet+}$ at 980 nm and $[C_{70}^{\bullet-}]_{max}$ was evaluated from isolated absorption at 1380 nm ($\varepsilon = 4000$ cm^{-1} mol^{-1} dm^3).[31] The Φ_{ET}^T values are listed in Table 3.

Since all Φ_{ET}^T values in Table 3 are less than 1, there are quenching processes other than electron transfer (Scheme 2), such as a collisional quenching process (k_{cq}^T), which may include deactivation via encounter complexes ($^3C_{60}$*···$(PTZ)_n$) or ($^3C_{70}$*···$(PTZ)_n$) and exciplexes [$^3(C_{60}^{\delta-}$···$(PTZ)_n^{\delta+})$*] or [$^3(C_{70}^{\delta-}$···$(PTZ)_n^{\delta+})$*] without forming detectable ions.[10]

Finally, the electron-transfer rate constants (k_{ET}^T) were calculated using $k_{ET}^T = \Phi_{ET}^T k_q^T$.[33,34] As listed in Table 3, the k_{ET}^T values were in the range of $(0.64–3.3) \times 10^9$ mol^{-1} dm^3 s^{-1}. These k_{ET}^T values are slightly smaller than k_{diff} in PhCN.[32] The order of the k_{ET}^T values is $(PTZ)_1 > (PTZ)_2 = (PTZ)_3$ for $^3C_{60}$* and $^3C_{70}$*. For each $(PTZ)_n$, the k_{ET}^T values for $^3C_{60}$* are larger than those for $^3C_{70}$*.

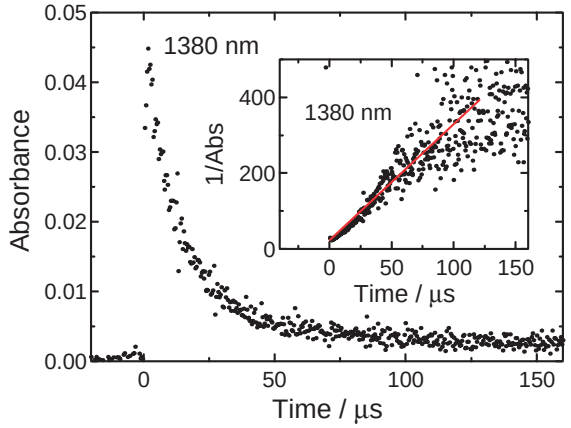

Fig. 6. Long time-scale decay of $C_{70}^{\bullet-}$ at 1380 nm produced by electron transfer from $(PTZ)_2$ via $^3C_{70}$* in Ar-saturated PhCN. Inset: Second-order plot.

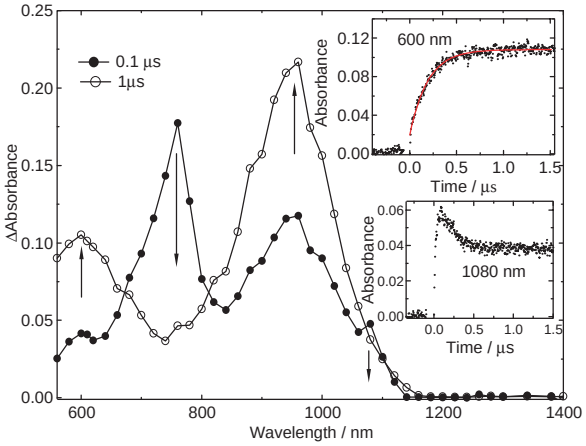

Fig. 7. Transient absorption spectra obtained by exciting with 532 nm laser light of C_{60} (0.15 mmol dm^{-3}) in the presence of $(PTZ)_3$ (2 mmol dm^{-3}) and HV^{2+} (2 mmol dm^{-3}) in Ar-saturated PhCN. Inset: Time profiles at 600 and 1080 nm.

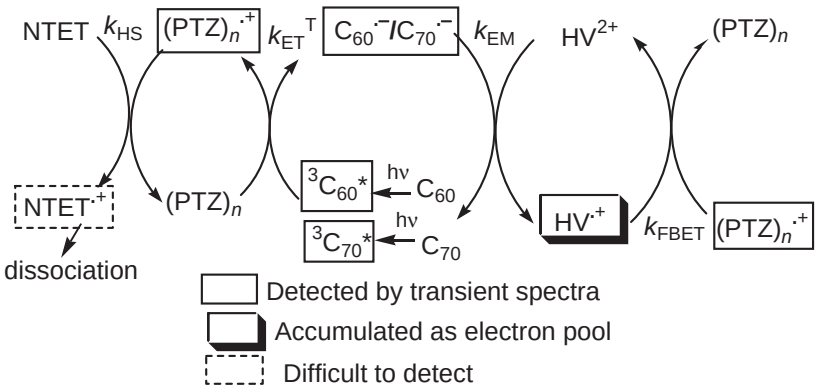

Scheme 3. Electron-mediating and hole-shifting system.

Back Electron Transfer Process. In longer timescale measurements, $C_{70}^{\bullet-}$ begins to decay after reaching a maximum intensity, as shown in Fig. 6 for $(PTZ)_2^{\bullet+}$. The second-order plot (1/Abs. vs. time) for the decay of $C_{70}^{\bullet-}$ was linear in the initial stage (inset of Fig. 6); however, the later stage contained much noise. Observed second-order kinetics indicate a bimolecular back electron transfer (BET) between from $C_{70}^{\bullet-}$ and $(PTZ)_n^{\bullet+}$ with the same concentration, returning to neutral molecules in their ground states (in Scheme 2). Bimolecular second-order kinetics also suggests that the back electron transfer takes place after the radical cation and radical anion are separately solvated as free radical ions. The slope of the second-order plot is k_{BET}/ε_A. Thus, on substituting the reported ε_A at 1380 nm for $C_{70}^{\bullet-}$, we could calculate the k_{BET} values, as listed in Table 3. Similar decay processes were observed for $C_{60}^{\bullet-}$ and $(PTZ)_n^{\bullet+}$. The k_{BET} values were in the range of $(0.81–2.8) \times 10^{10}$ mol^{-1} dm^3 s^{-1}, which are slightly larger than the k_{diff} value, probably due to uncertainty in the analysis. Although $k_{BET} > k_{ET}^T$, the actual rates of the forward process should be faster than that of the backward process, because the concentrations of neutral $(PTZ)_n$s were much higher than those of $(PTZ)_n^{\bullet+}$, even though the concentration of $C_{60}^{\bullet-}$ (or $C_{70}^{\bullet-}$) was similar to that of $^3C_{60}$* (or $^3C_{70}$*).

Electron-Mediating System. The addition of HV^{2+} to a mixture of C_{60} and $(PTZ)_3$ gave rise to the transient absorption spectra after laser light excitation of C_{60} shown in Fig. 7. Along with the rapid decay of the $^3C_{60}$* band at 740 nm and the corresponding rapid increase in the $C_{60}^{\bullet-}$ (1080 nm) and $(PTZ)_3^{\bullet+}$ (800–1100 nm) bands, the absorption band for $HV^{\bullet+}$ appeared at 600 nm. The formation rate of $HV^{\bullet+}$ was almost the same as decay rate of $C_{60}^{\bullet-}$, as shown in the inset of Fig. 7. These observations suggest that $HV^{\bullet+}$ is produced via an electron-mediating process from $C_{60}^{\bullet-}$ to HV^{2+}.[35] The E_{red} of HV^{2+} (−0.65 V vs. Ag/Ag$^+$ in PhCN) also suggests that this process can occur at room temperature. For C_{70} and $(PTZ)_n$, almost the same results were obtained. These observations clearly demonstrate that these photosensitized electron-transfer/electron-mediating processes are induced by the photoexcitation of C_{60}/C_{70}, as shown in Scheme 3, in which k_{EM} refers to the rate constant for the electron-mediating process. The k_{EM} value was evaluated to be 2.6×10^9 mol^{-1} dm^3 s^{-1} in PhCN from the increase in the band for $HV^{\bullet+}$ at different concentrations of HV^{2+}.

In longer timescale measurements, the absorption intensity of $HV^{\bullet+}$ at 600 nm began to decay after reaching a maximum at 1 μs (Fig. 8). Plot of the reciprocal of the absorbance vs.

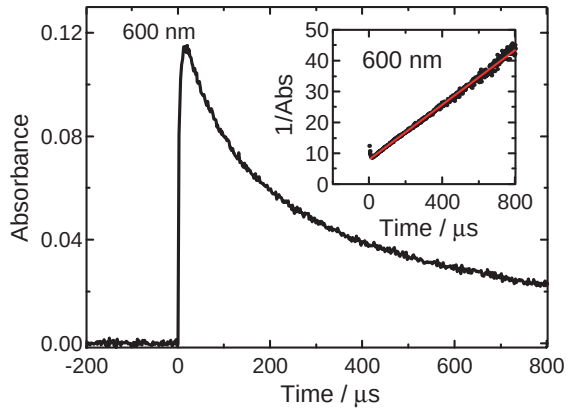

Fig. 8. Long-timescale decay of $HV^{\bullet+}$ at 600 nm produced by electron-mediating process from $C_{60}^{\bullet-}$ to HV^{2+} in the presence of $(PTZ)_3^{\bullet+}$ in Ar-saturated PhCN. Inset. Second-order plot.

time gave a straight line, which indicates that $HV^{\bullet+}$ decays following second-order kinetics. This suggests that $HV^{\bullet+}$ decays due to final back electron transfer (FBET) from $HV^{\bullet+}$ to $(PTZ)_3^{\bullet+}$ (Scheme 3); the rate constant k_{FBET} was estimated to be 3.0×10^8 mol^{-1} dm^3 s^{-1}. This value is smaller than the k_{BET} value between $C_{60}^{\bullet-}$ with $(PTZ)_3^{\bullet+}$ (2.0×10^{10} mol^{-1} dm^3 s^{-1}) by a factor of ca. 1/70, because FBET between the positively charged species must be slower than that between the oppositely charged species.

After adding 2,2′,2″-nitrilotriethanol (NTET) to a solution containing C_{60}, $(PTZ)_3$, and HV^{2+} in PhCN, the characteristic absorption band for $HV^{\bullet+}$ observed at 600 nm after laser excitation of C_{60} did not decay even in long timescale measurements. Thus, the steady-state photolysis of C_{60} using light with a wavelength longer than 430 nm was performed in the presence of $(PTZ)_3$, HV^{2+}, and NTET in PhCN. With an increase in the irradiation time, a progressive increase in the $HV^{\bullet+}$ band at 600 nm was observed, as shown in Fig. 9, suggesting that $(PTZ)_3^{\bullet+}$, which is the counter part of $HV^{\bullet+}$ in the FBET process, is removed by addition of NTET, due to hole shifting (k_{HS}) from $(PTZ)_n^{\bullet+}$ to NTET; then, $HV^{\bullet+}$ accumulated. Similar phenomena were observed for C_{70} and $(PTZ)_n$. As shown in Scheme 3, the accumulation of $HV^{\bullet+}$ occurs due to photoexcitation of C_{60}/C_{70} accompanied by photosensitized-electron-transfer, electron-mediating, and hole-transfer processes.

Conclusion

In the present study, we showed that C_{60} and C_{70} act as good photosensitizing electron acceptors in the presence of phenothiazine oligomers $(PTZ)_n$s, which were also proven to be good electron donors. Their transient species, such as triplet excited states of C_{60}/C_{70} and the ion radicals of C_{60}/C_{70} and $(PTZ)_n$s, were well characterized by using transient absorption spectroscopy in the near-IR region. The structures of $(PTZ)_2^{\bullet+}$ and $(PTZ)_3^{\bullet+}$ generated within 100 ns through intermolecular photoinduced electron transfer reactions were found to be identical to those of the most stable radical cations in the steady-state. The order of the rates of electron transfer via $^3C_{60}$* and $^3C_{70}$* is $(PTZ)_1 > (PTZ)_2 = (PTZ)_3$, which follows the decrease in their oxidation potentials. Upon addition of the viologen dication and a sacrificial donor, a photosensitizing electron-transfer/electron-mediating cycle was established, giving rise to a prolonged lifetime for the viologen radical cation, making it an electron pool, which should be useable as source of excess electrons in photovoltaic cells and H_2-evolution reactions.

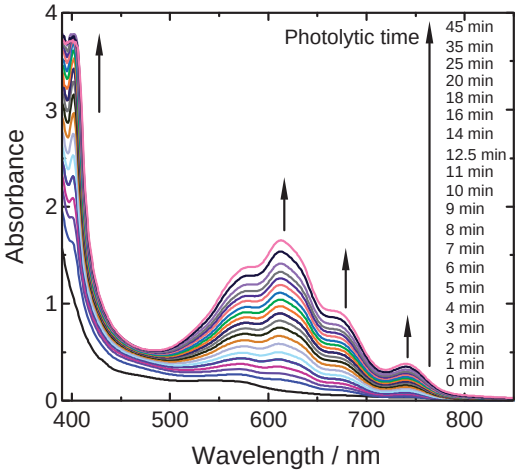

Fig. 9. Steady-state absorption spectra obtained by photolysis of C_{60} (0.15 mmol dm^{-3}) with light longer than 500 nm in presence of $(PTZ)_3$ (2 mmol dm^{-3}), HV^{2+} (2 mmol dm^{-3}), and NTET (0.5 mol dm^{-3}) in Ar-saturated PhCN.

Experimental

Materials. C_{60} was obtained from Texas Fullerenes Corporation with a purity of 99.9%. $(PTZ)_3$ was prepared as described previously.[22] $(PTZ)_2$ is a known compound[36] and prepared from 3-(10-phenothiazinyl)phenothiazine[37] through *N*-phenylation via Pd^0-mediated cross-coupling.[21,23] Hexylviologen dication (HV^{2+}) was used as a perchlorate salt. PhCN, used as a solvent, was of HPLC grade and used as received.

Preparation of $(PTZ)_2^{\bullet+}PF_6^-$. Phenothiazine dimer, 3-(10-phenothiazinyl)phenothiazine,[37] (32.0 mg, 0.0677 mmol) was dissolved in dichloromethane (8 mL). Tris-*p*-bromophenylaminium hexafluorophosphate ($TBPA^+PF_6^-$, 43.0 mg, 0.0686 mmol) was separately dissolved in dichloromethane (8 mL). The solution of $TBPA^+PF_6^-$ was added slowly to the solution of $(PTZ)_2$ at room temperature with stirring in a glove box. After 30 min, the solvent of the reaction mixture was evaporated under reduced pressure. The residue was dissolved in dichloromethane (2 mL), and then, diethyl ether (40 mL) was added. The precipitate $(PTZ)_2^{\bullet+}PF_6^-$ was collected as a deep blue powder (28.1 mg, 67%). Vis and near-IR absorption: λ_{max} (ε): 394 (4990), 448 (4129), 610 (6440), 990 nm (10600) in CH_2Cl_2, 396 (4550), 449 (3620), 612 (5280), 676 (5530), 980 nm (8600) in PhCN. $(PTZ)_2^{\bullet+}PF_6^-$: $C_{30}H_{20}F_6N_2PS_2$; MW 617.59; decomp. ca. 150 °C; MS (FAB): m/z 472 ($[C_{30}H_{20}N_2S_2]^+$), 145 ($[PF_6]^-$); IR (KBr, cm^{-1}): 1604, 1560, 1489, 1458, 1350, 1258, 1165, 1132, 1086, 839, 756, 557; Anal. Calcd for $(PTZ)_2^{\bullet+}PF_6^- \cdot 0.4H_2O$: Calcd: C, 57.67; H, 3.36; N, 4.48%. Found C, 57.86; H, 3.61; N, 4.39%. ESR $g = 2.0044$ ($\nu_0 = 9.4408$ GHz), $a_N = 0.67$ mT, $a_H = 0.39$ mT, $a_H = 0.20$ mT) in butyronitrile at room temperature.

Apparatus. Redox potentials were measured on a voltammetric analyzer (BAS CV-50W) in a conventional three electrode-cell equipped with Pt-working and counter electrodes and with an Ag/AgCl reference electrode at a scan rate of 100 mV s^{-1}. In each

case, the solutions contained 0.1 mol dm^{-3} of tetrabutylammonium perchlorate (Nakalai Tesque) as the electrolyte and were deaerated with Ar-bubbling before measurements.

Steady-state absorption spectra were measured on a JASCO/V-570 spectrophotometer. The absorption spectra of the isolated radical cations of $(PTZ)_n$s were measured using a 2-mm cell.

Transient absorption spectra in the vis/near-IR regions were obtained by using a laser-flash photolysis apparatus. In the mixtures containing C_{60}, C_{70}, $(PTZ)_n$, and HV^{2+}, C_{60} and C_{70} were excited with the SHG (532 nm) light of a Nd:YAG laser (Quanta-Ray; 6 ns fwhm). A Ge-APD module (600–1600 nm) was employed as a detector for monitoring the light from a pulsed Xe-lamp.[38] For measurements with a timescale longer than 10 μs, an InGaAs-PIN photodiode was used as a detector for monitoring light from a continuous Xe-lamp (150 W).[39] The sample solutions were deaerated by bubbling with argon gas before measurements. Laser photolysis was performed on solutions in a rectangular quartz cell with a 10-mm optical path. All the measurements were carried out at 23 °C.

References

1 C. S. Foote, in *Physics and Chemistry of the Fullerenes*, ed. by K. Prassides, Kluwer, Academic Publisher, Dordrecht, **1994**, NATO ASI Series Vol. C-443, pp. 79–96.

2 O. Ito, *Res. Chem. Intermed.* **1997**, *23*, 389.

3 M. Maggini, D. M. Guldi, in *Molecular and Supramolecular Photochemistry*, ed. by V. Ramamurthy, K. S. Schanze, Marcel Dekker, New York, **2000**, Vol. 4, pp. 149–196.

4 D. M. Guldi, P. V. Kamat, in *Fullerenes, Chemistry, Physics and Technology*, ed. by K. M. Kadish, R. S. Ruoff, Wiley-Interscience, New York, **2000**, pp. 225–281.

5 J. W. Arbogast, C. S. Foote, *J. Am. Chem. Soc.* **1991**, *113*, 8886.

6 R. J. Sension, A. Z. Szarka, G. R. Smith, R. M. Hochstrasser, *Chem. Phys. Lett.* **1991**, *185*, 179.

7 S. Fukuzumi, T. Suenobu, M. Patz, T. Hirasaka, S. Itoh, M. Fujitsuka, O. Ito, *J. Am. Chem. Soc.* **1998**, *120*, 8060.

8 H. Onodera, Y. Araki, M. Fujitsuka, S. Onodera, O. Ito, F. Bai, M. Zheng, J.-L. Yang, *J. Phys. Chem. A* **2001**, *105*, 7341.

9 O. Ito, Y. Sasaki, M. E. El-Khouly, Y. Araki, M. Fujitsuka, A. Hirao, H. Nishizawa, *Bull. Chem. Soc. Jpn.* **2002**, *75*, 1247.

10 A. S. D. Sandanayaka, Y. Araki, C. Luo, M. Fujitsulka, O. Ito, *Bull. Chem. Soc. Jpn.* **2004**, *77*, 1313.

11 H. N. Ghosh, H. Pal, A. V. Sapre, J. P. Mittal, *J. Am. Chem. Soc.* **1993**, *115*, 11722.

12 Y. Yahata, Y. Sasaki, M. Fujitsuka, O. Ito, *J. Photosci.* **2000**, *6*, 117.

13 H. Yonemura, N. Kuroda, S. Moribe, S. Yamada, *C. R. Chim.* **2006**, *9*, 254.

14 Y. Sasaki, Y. Araki, O. Ito, M. M. Alam, *Photochem. Photobiol. Sci.* **2007**, *6*, 560.

15 A. Higuchi, H. Inada, T. Kobata, Y. Shirota, *Adv. Mater.* **1991**, *3*, 549.

16 R. Y. Lai, E. F. Fabrizio, L. Lu, S. A. Jenekhe, A. J. Bard, *J. Am. Chem. Soc.* **2001**, *123*, 9112.

17 M. M. Alam, S. A. Jenekhe, *Chem. Mater.* **2002**, *14*, 4775.

18 D.-H. Hwang, S.-K. Kim, M.-J. Park, J.-H. Lee, B.-W. Koo, I.-N. Kang, S.-H. Kim, T. Zyung, *Chem. Mater.* **2004**, *16*, 1298.

19 M. M. Alam, C. J. Tonzola, S. A. Jenekhe, *Macromolecules* **2003**, *36*, 6577.

20 R. Argazzi, C. A. Bignozzi, T. A. Heimer, F. N. Castellano, G. J. Meyer, *J. Phys. Chem. B* **1997**, *101*, 2591.

21 T. Okamoto, M. Kozaki, M. Doe, M. Uchida, G. Wang, K. Okada, *Chem. Mater.* **2005**, *17*, 5504.

22 E. Wagner, S. Filipek, M. K. Kalinowski, *Monatsh. Chem.* **1988**, *119*, 929.

23 T. Okamoto, M. Kuratsu, M. Kozaki, K. Hirotsu, A. Ichimura, T. Matsushita, K. Okada, *Org. Lett.* **2004**, *6*, 3493.

24 M. J. Frisch, G. W. Trucks, H. B. Schlegel, G. E. Scuseria, M. A. Robb, J. R. Cheeseman, J. A. Montgomery, Jr., T. Vreven, K. N. Kudin, J. C. Burant, J. M. Millam, S. S. Iyengar, J. Tomasi, V. Barone, B. Mennucci, M. Cossi, G. Scalmani, N. Rega, G. A. Petersson, H. Nakatsuji, M. Hada, M. Ehara, K. Toyota, R. Fukuda, J. Hasegawa, M. Ishida, T. Nakajima, Y. Honda, O. Kitao, H. Nakai, M. Klene, X. Li, J. E. Knox, H. P. Hratchian, J. B. Cross, C. Adamo, J. Jaramillo, R. Gomperts, R. E. Stratmann, O. Yazyev, A. J. Austin, R. Cammi, C. Pomelli, J. W. Ochterski, P. Y. Ayala, K. Morokuma, G. A. Voth, P. Salvador, J. J. Dannenberg, V. G. Zakrzewski, S. Dapprich, A. D. Daniels, M. C. Strain, O. Farkas, D. K. Malick, A. D. Rabuck, K. Raghavachari, J. B. Foresman, J. V. Ortiz, Q. Cui, A. G. Baboul, S. Clifford, J. Cioslowski, B. B. Stefanov, G. Liu, A. Liashenko, P. Piskorz, I. Komaromi, R. L. Martin, D. J. Fox, T. Keith, M. A. Al-Laham, C. Y. Peng, A. Nanayakkara, M. Challacombe, P. M. W. Gill, B. Johnson, W. Chen, M. W. Wong, C. Gonzalez, J. A. Pople, *Gaussian 03, Revision B.04*, Gaussian Inc., Pittsburgh PA, **2003**.

25 D. Rehm, A. Weller, *Isr. J. Chem.* **1970**, *8*, 259.

26 M. M. Alam, A. Watanabe, O. Ito, *J. Photochem. Photobiol., A* **1997**, *104*, 59.

27 J. W. Arbogast, C. S. Foote, M. Kao, *J. Am. Chem. Soc.* **1992**, *114*, 2277.

28 H. T. Etheridge, III, B. R. Weisman, *J. Phys. Chem.* **1995**, *99*, 2782.

29 T. Nojiri, M. M. Alam, H. Konami, A. Watanabe, O. Ito, *J. Phys. Chem. A* **1997**, *101*, 7943.

30 M. Fujitsuka, C. Luo, O. Ito, *J. Phys. Chem. B* **1999**, *103*, 445.

31 M. M. Alam, A. Watanabe, O. Ito, *Bull. Chem. Soc. Jpn.* **1997**, *70*, 1833.

32 S. I. Murov, I. Carmichael, G. L. Hug, *Handbook of Photochemistry*, Marcel-Dekker, New York, **1993**.

33 C. A. Steren, H. van Willigen, L. Biczók, N. Gupta, H. Linschitz, *J. Phys. Chem.* **1996**, *100*, 8920.

34 K. Yamanaka, M. Fujitsuka, O. Ito, T. Aoshima, T. Fukushima, T. Miyashi, *Bull. Chem. Soc. Jpn.* **2003**, *76*, 1341.

35 T. Konishi, M. Fujitsuka, O. Ito, Y. Toba, Y. Usui, *J. Phys. Chem. A* **1999**, *103*, 9938.

36 M. V. Diudea, *Tetrahedron Lett.* **1982**, *23*, 1367.

37 Y. Tsujino, *Tetrahedron Lett.* **1968**, *9*, 2545.

38 K. Matsumoto, M. Fujitsuka, T. Sato, S. Onodera, O. Ito, *J. Phys. Chem. B* **2000**, *104*, 11632.

39 T. Nakamura, J. Ikemoto, M. Fujitsuka, Y. Araki, O. Ito, K. Takimiya, Y. Aso, T. Otsubo, *J. Phys. Chem. B* **2005**, *109*, 14365.